

Innovative flow-through reaction system for the sustainable production of phenolic monomers from lignocellulose catalyzed by supported Mo₂C.

Maitane Maisterra,^[a] María Atienza-Martínez,^[a] Karina Hablich,^[a] Rui Moreira,^[b] Víctor Martínez-Merino,^[a] Luis M. Gandía,^[a] Alfonso Cornejo,^{*[a]} and Fernando Bimbela^{*[a]}

Molybdenum carbide supported on activated carbon (β -Mo₂C/AC) has been tested as catalyst in the reductive catalytic fractionation (RCF) of lignocellulosic biomass both in batch and in Flow-Through (FT) reaction systems. High phenolic monomer yields (34 wt.%) and selectivity to monomers with reduced side alkyl chains (up to 80 wt.%) could be achieved in batch in the presence of hydrogen. FT-RCF were made with no hydrogen feed, thus *via* transfer hydrogenation from ethanol. Similar selectivity could be attained in FT-RCF using high catalyst/biomass ratios (0.6) and high molybdenum loading (35 wt.%) in the catalyst, although selectivity decreased with lower catalyst/biomass ratios or molybdenum contents. Regardless of these

parameters, high delignification of the lignocellulosic biomass and similar monomer yields were observed in the FT mode (13–15 wt.%) while preserving the holocellulose fractions in the delignified pulp. FT-RCF system outperforms the batch reaction mode in the absence of hydrogen, both in terms of activity and selectivity to reduced monomers that is attributed to the two-step non-equilibrium processes and the removal of diffusional limitations that occur in the FT mode. Even though some molybdenum leaching was detected, the catalytic performance could be maintained with negligible loss of activity or selectivity for 15 consecutive runs.

Introduction

Lignocellulosic biomass is one of the most widely available sources of renewable matter. Biomass from forestry sources is mainly constituted by three components, cellulose (40–60 wt.%), hemicellulose (10–40 wt.%) and lignin (15–30 wt.%), the proportions of which vary depending on the species. Lignin is deemed as the largest renewable source of aromatic building blocks.^[1] Therefore, fractionation of lignocellulose is of key importance to recover valuable building blocks, commodities and value-added chemical compounds.^[2,3] It can contribute not only to the economic and environmental viability of biorefineries, but also to the development of new sustainable

strategies for the synthesis of renewable aromatics, as an alternative to petrochemical industry.^[4]

Many studies have focused on the valorisation of lignin-rich streams (often referred to as 'technical lignins') derived from different biomass fractionation processes to obtain value-added products.^[5] Nevertheless, lignin depolymerization yields to monomeric phenols are usually low because of the chemical modification of lignin's native structure upon its isolation by physicochemical and thermochemical pre-treatments.^[1,6]

During the last years, 'lignin-first' strategies,^[7] which are commonly based in the so called Reductive Catalytic Fractionation (RCF) process,^[8] have emerged as an alternative to the traditional biorefinery approaches. Delignification of the raw material is firstly conducted by thermal and solvolytic disassembly of lignin without altering its native structure,^[9] and then metal-catalysed hydrogenolysis mainly acts on aryl ether bonds, primarily on β -O-4. Simultaneously, the most reactive intermediates obtained in lignin depolymerization, mainly olefins and carbonyls that often lead to repolymerization phenomena,^[10] are stabilized by reductive processes in the presence of catalysts such as Ru/C,^[7] Pd/C^[11] and Ni/Al₂O₃.^[12] As a result, higher yields of chemically stable phenolic compounds are obtained. Although some attempts have been made, recovery of the catalyst after batch RCF is still a major issue to be solved, since catalyst particles end up mixed with the delignified pulp after reaction.^[12,13]

The development of flow-through (FT) reaction systems to conduct lignin RCF while allowing catalyst recovery is an interesting alternative. Furthermore, this approach is of great interest for scaling-up these processes at industrially-relevant scales. Some relevant studies have been already published on

[a] M. Maisterra, M. Atienza-Martínez, K. Hablich, V. Martínez-Merino, L. M. Gandía, A. Cornejo, F. Bimbela
Institute for Advanced Material and Mathematics (INAMAT²) - Department of Sciences
Universidad Pública de Navarra
Ed. 'Los Acebos', Campus de Arrosadía S/N, 31006 Pamplona, Spain
E-mail: alfonso.cornejo@unavarra.es
fernando.bimbela@unavarra.es

[b] R. Moreira
CIEPQPF, FCTUC, Department of Chemical Engineering
University of Coimbra
Rua Sílvio Lima, Pólo II - Pinhal de Marrocos, Coimbra, Portugal

Supporting information for this article is available on the WWW under <https://doi.org/10.1002/cssc.202301591>

© 2024 The Authors. ChemSusChem published by Wiley-VCH GmbH. This is an open access article under the terms of the Creative Commons Attribution Non-Commercial NoDerivs License, which permits use and distribution in any medium, provided the original work is properly cited, the use is non-commercial and no modifications or adaptations are made.

the continuous-flow solvolysis of downstream lignins from the pulp and paper industry.^[14,15] However, very few studies have been reported on flow-through Reductive Catalytic Fractionation (FT-RCF) to date. Amongst them, a semi-continuous dual-bed flow reactor with Ni/C as catalyst has been reported with the catalyst being used in four consecutive runs while maintaining reasonable selectivity levels to saturated compounds, though a noticeable decay in selectivity could be observed after each use.^[16] Nonetheless, the physical separation of the feedstock and the catalyst not only allowed to study the two independent processes taking place in RCF, lignin solvolysis and hydrogenolysis, but also their separate optimization,^[17] reaching up to 23 wt.% of monomer yield using a pelletized Ni/C catalyst.^[18] Some authors concluded that delignification proceeded much faster than the hydrogenolysis process using a Pd/C catalyst.^[19] Indeed, up to 37–40 wt.% of monomers, which is very close to the theoretical maximum yield, can be obtained in the presence of Pd/C, though having a noticeable contribution of hemicelluloses as reducing agent.^[20]

Transition metal carbide catalysts, which are usually prepared using activated carbons (AC) as supports, have shown to be stable against deactivation by massive coke formation, which is presently the main setback in catalytic hydrogenolysis of lignin. α -MoC_{1-x}/AC has been used in the depolymerization of Kraft lignin.^[21] It has also been reported that β -Mo₂C/AC presents remarkable activity in the depolymerization of Kraft lignin from wheat straw at 280 °C in ethanol.^[22] Recently, the utilization of molybdenum carbide immobilized on carbon nanotubes, Mo₂C/CNT, has been described in the RCF of apple tree wood.^[23]

In this study we present a FT-RCF reaction in which a forestry industry residue, poplar sawdust, was used as feedstock and a transition metal carbide as catalyst, β -Mo₂C/AC. The catalytic performance in RCF attained using FT mode was compared to the results obtained in batch. The FT reaction system was extremely simple, and consisted in a dual fixed-bed configuration and flowing ethanol as reaction medium in the absence of hydrogen. FT configurations clearly outperforms the classical batch results even using relatively low catalyst-to-biomass mass ratios (0.3 and 0.6). Both activity and selectivity of the catalyst in FT and batch were close to those achieved using the benchmark Ru/C catalyst. This set-up for the FT-RCF allowed easy reuse of the catalyst in 15 consecutive cycles. To the best of our knowledge, this is the most extensive catalyst recycling in FT-RCF of biomass ever reported to date, and the first report on FT-RCF using β -Mo₂C/AC.

Results and Discussion

Catalyst characterization

Two sets of β -Mo₂C/AC were synthesized with different nominal Mo contents: 5 wt.% and 35 wt.% (see Experimental Section). Hereafter, the catalyst samples will be denoted as 5-Mo₂C/AC and 35-Mo₂C/AC. The actual Mo content in the samples was determined by means of inductively coupled plasma – optical

emission spectroscopy (ICP-OES). The results obtained (see Table S1) show a good concordance between the nominal and the actual contents. Scanning Transmission Electronic Microscopy (STEM) images of 35-Mo₂C/AC showed the presence of Mo₂C nanoparticles as irregular agglomerates, with a broad size distribution around 30–32 nm (see Figure 1 and Figure S1), although some smaller nanoparticles were also present. The presence of Mo was confirmed by Energy-dispersive X-ray spectroscopy (EDS) analyses. These large agglomerates are consistent with the reduction of the surface area from 880 m²/g in the parent AC, to 746 m²/g in 5-Mo₂C/AC, and 439 m²/g in 35-Mo₂C/AC catalysts (Table S2). Pore volume also decreased with increasing Mo loading (0.69 cm³/g, 0.58 cm³/g and 0.35 cm³/g for AC, 5-Mo₂C/AC and 35-Mo₂C/AC, respectively). X-ray photoelectron spectroscopy (XPS) analyses of 35-Mo₂C/AC (Figure 1) evidenced the presence of surface molybdenum and oxygen atoms, the latter because of the passivation process. Fitting of the Mo region in XPS analyses (228–237 eV) was consistent with the contribution of Mo (II) as Mo₂C (Mo 3d¹ ca. 7.4%). Higher oxidation state for Mo was found, MoO₂ (3d² and 3d³, 14.91%), and Mo (VI), which is compatible with MoO₃ species (3d⁴, 77.67%) that is expected after the passivation process upon catalyst preparation. The X-ray diffraction (XRD) pattern of the as-prepared catalyst confirmed the presence of Mo₂C in its β phase on the activated carbon in 35-Mo₂C/AC (JCPDS PDF 11–0680, Figure 1). 5-Mo₂C/AC (Figure S2) presented a similar pattern although signals corresponding to Mo₂C in its β phase appeared as shoulders due to the higher dispersion and smaller particle size of β -Mo₂C. A broad shoulder in the range of 20–30° confirmed in both cases the presence of graphite in the solid.

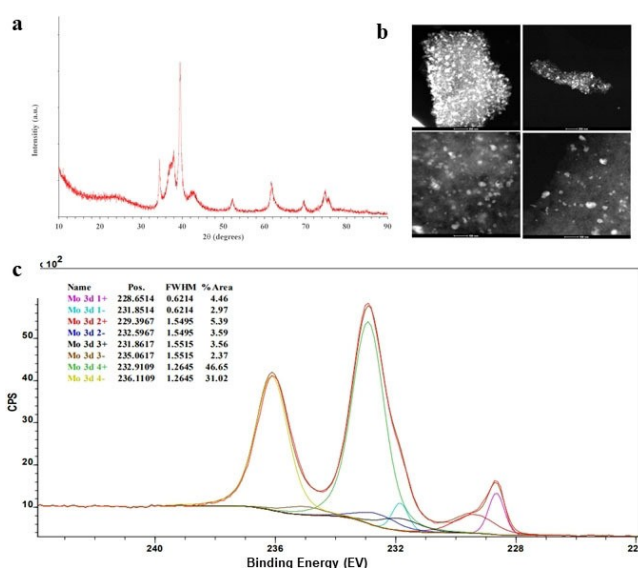


Figure 1. Characterization results of fresh 35-Mo₂C/AC: a) XRD pattern, b) STEM images and c) XPS spectrum and its fitting by curve deconvolution.

Batch Reductive Catalytic Fractionation

Depolymerization of ethanosolv lignin obtained from poplar sawdust^[24] was tried using 35-Mo₂C/AC in ethanol at 200 °C. Too high reactivity was observed. Indeed, most of the reaction products could not be properly identified. Therefore, the depolymerization of this technical lignin was abandoned and ethanosolv lignin was only used as a reference for the solvolytic step in the RCF process.

35-Mo₂C/AC was tested in the RCF of poplar sawdust at 200 °C after 150 min in ethanol under hydrogen (Table 1, run code 35b, Figure S3). The monomer yield referred to the lignin content in the feedstock (Table S3) reached 17 wt.%, which was similar to that of the run conducted with the reference catalyst, Ru/C (20 wt.%), denoted as Rua in Table 1, and with similar monomer distribution in both cases (see Figure 2a). Main monomers found throughout this work are shown and identified in Figure 2.

The effects of the solvent, temperature and reaction time on monomer yield and distribution were further evaluated in the RCF of poplar sawdust using the 35-Mo₂C/AC catalyst (Figure 2a and Figure S3). Monomer yield decreased from 17 wt.% (run 35b, 200 °C, 150 min) to 9.7 wt.% when reaction temperature decreased to 150 °C even after much longer reaction time (run 35a), but when the temperature was raised to 250 °C (run 35h), the monomer yield was 16 wt.%. The monomers yield steadily increased with reaction time at 200 °C (17 wt.%, 26 wt.% and 34 wt.% in runs 35b, 35c and 35d, respectively), and then decreased at longer reaction times (29 wt.% and 28 wt.%, runs 35f and 35g). Monomer yield reached its maximum in run 35d (ca. 34 wt.%) and then decreased at longer reaction times, which evidenced repolymerization of the monomers.^[23] It must be highlighted that, in the absence of hydrogen (run 35e), the monomer yield was only 8.7 wt.%.

The effect of the solvent was also tested at 200 °C under hydrogen atmosphere using 35-Mo₂C/AC (Figure S3b) in meth-

anol, propan-2-ol and butan-1-ol (runs 35i, 35j and 35k, respectively). Monomer yields in 35i (7.3 wt.%) or 35j and 35k (8.8 wt.% and 26.8 wt.%,) were much lower than in 35d (34 wt.%). These results reveal that the choice of the solvent is not trivial. Short-chain linear alcohols promote lignin solvolysis and thereby delignification of the biomass. This is in agreement with previous studies using methanol.^[25,26] Finally, RCF was carried out with the 5-Mo₂C/AC catalyst (run 5d, Ethanol, 200 °C, H₂), under the reaction conditions that provided the best yields in the previous runs (run 5d, ethanol, 200 °C, H₂), yielding 13 wt.% of monomeric phenols (Figure 2a).

The selectivity of the different Mo catalysts was also evaluated. The combined amount of methylsyringol (S1) and propenylsyringol (S4) was in the range of 60 wt.% when RCF was performed in the presence of 35-Mo₂C/AC and under hydrogen atmosphere, but it decreased to 36 wt.% when ethanol was the sole hydrogen source (run 35e). Similarly, the combined amount of propylsyringol (S3) and propenylsyringol (S4) was in the 40–50 wt.% range, being S4 the major monomer (ca. 35–40 wt.%). It is worth noting that, when RCF was run either in the absence of hydrogen (35e) or with a lower catalyst load (5d) the amount of more oxidized species such as 4-(2-oxo-propyl)-guaiacol (G5) increased up to 25 wt.%, which evidenced the role of Mo as catalysts and hydrogen as reducing agent in the reductive processes of the alkyl-side chain.

Mass distribution of ethanosolv lignin and Lignin Depolymerized Oil (LDO) obtained after RCF using 35-Mo₂C/AC and 5-Mo₂C/AC were compared using Size Exclusion Chromatography (SEC, Figure 2b). Ethanosolv lignin presented a broad mass distribution from 500 Da to 1000 Da, with some fractions at 404 Da and 625 Da. The best fractionation of the solvolytic lignin was attained when RCF was carried in ethanol at 200 °C using 35-Mo₂C/AC, where the prevalent mass corresponded to monomers. The major peak appeared at ca. 150 Da, together with two shoulders at ca. 105 Da and 235 Da. Peaks corresponding to dimers, trimers and tetramers (450 Da and 690 Da) were much less important than the former one, and masses higher

Table 1. Reaction conditions for the different batch RCF runs.

Run	Catalyst	Solvent	Temperature (°C)	Time (Min)	Atm. (30 bar)
Rua	Ru/C	Ethanol	200	150	H ₂
Rub	Ru/C	Ethanol	250	150	H ₂
35a	35-Mo ₂ C/AC	Ethanol	150	1350	H ₂
35b	35-Mo ₂ C/AC	Ethanol	200	150	H ₂
35c	35-Mo ₂ C/AC	Ethanol	200	240	H ₂
35d	35-Mo ₂ C/AC	Ethanol	200	480	H ₂
35e	35-Mo ₂ C/AC	Ethanol	200	480	N ₂
35f	35-Mo ₂ C/AC	Ethanol	200	990	H ₂
35g	35-Mo ₂ C/AC	Ethanol	200	1350	H ₂
35h	35-Mo ₂ C/AC	Ethanol	250	150	H ₂
35i	35-Mo ₂ C/AC	Methanol	200	120	H ₂
35j	35-Mo ₂ C/AC	Propan-2-ol	200	480	H ₂
35k	35-Mo ₂ C/AC	Butan-1-ol	200	480	H ₂
5d	5-Mo ₂ C/AC	Ethanol	200	480	H ₂

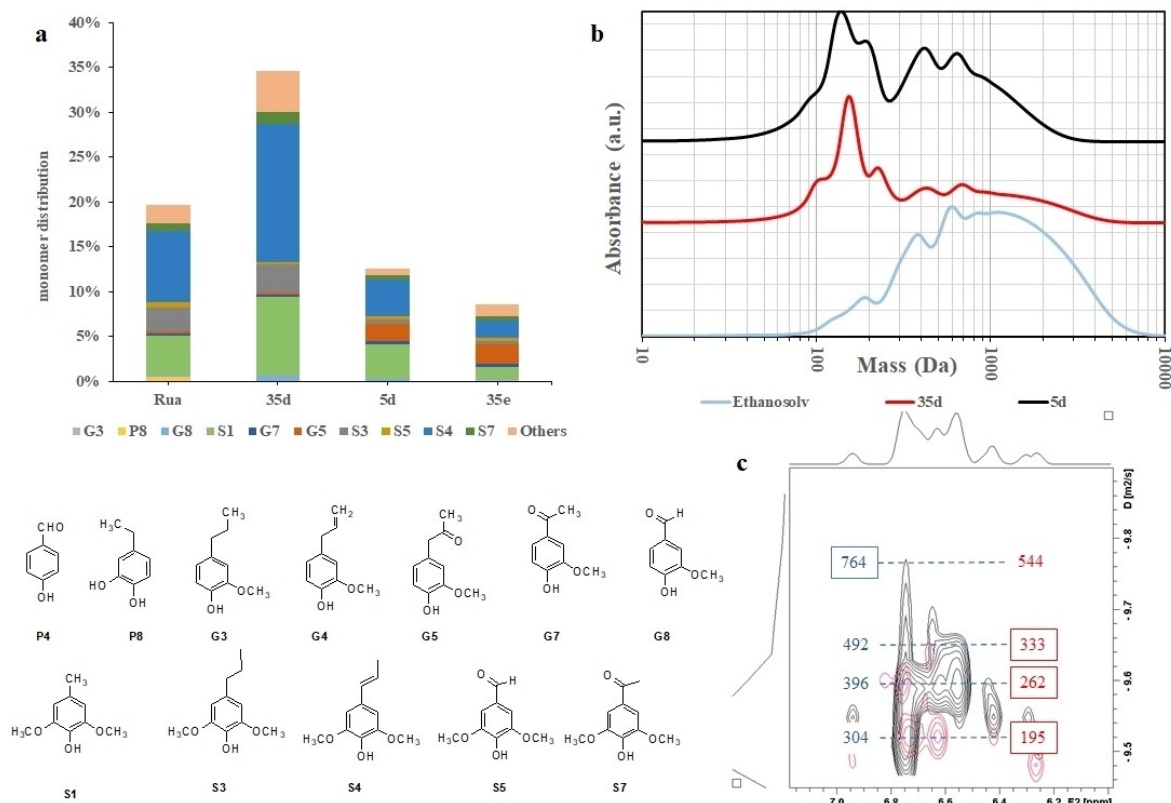


Figure 2. a) Monomer distribution and main monomers for poplar sawdust in runs Rua, 35d, 5d and 35e (see Table 1). b) SEC chromatograms for ethanosolv lignin and LDO from RCF in runs 35d (red) and 5d (black). c) DOSY spectra for RCF runs 35d (red) and 5e (black). Apparent mass values in DOSY spectra were estimated using PS calibration (blue figures) and PEG calibration (red figures).^[24]

than 1000 Da were barely observed. Other solvents or reaction conditions using 35-Mo₂C/AC (Figure S3) produced LDO where dimers and trimers were much more prevalent and masses beyond 1000 Da could be found, evidencing that either depolymerization was less efficient, or some repolymerization took place. When 5-Mo₂C/AC was used, although the peak corresponding to monomers at 150 Da was the most intense, those corresponding to dimers and trimers and a broad shoulder for oligomers were much more important than in the presence of 35-Mo₂C/AC. Therefore, mass distribution was narrower when 35-Mo₂C/AC was used, regardless of the solvent and the reaction conditions (see Figure S3). Diffusion Ordered Nuclear Magnetic Resonance spectroscopy (DOSY-NMR) (Figure 2d and S3c) confirmed that depolymerization was much more efficient in the presence of 35-Mo₂C/AC than using 5-Mo₂C/AC (Figure S3e).

Catalyst recovery from the delignified sawdust pulp after RCF was attempted by physical separation following a procedure described in the literature.^[7] The recovered material was tested under the same reaction conditions as those used with the fresh catalyst (200 °C, ethanol), providing again good monomer yields after 240 min (26 wt.%), and a similar monomer distribution than that obtained with the fresh catalyst. SEC analyses (Figure S4), however, showed that depolymerization was less efficient, as the presence of trimers and dimers was more significant. Additionally, only 25% of the initial catalyst

mass was recovered while the rest remained in the delignified pulp, which evidenced the inadequacy of this methodology for catalyst recovery.

Flow-Through Reductive Catalytic Fractionation (FT-RCF)

As discussed above, problems associated to catalyst recovery in batch RCF can be circumvented using FT-RCF. A laboratory scale FT-RCF was set-up. The FT system (See Experimental section and Figure S5) consisted of a liquid feeding system and two stainless-steel tubular reactors connected in series for placing two separate beds, both having a fixed-bed reactor configuration (the first for the biomass feedstock, and the second for the catalyst bed) that were placed in a reaction oven. The pressure was controlled using a back-pressure regulator downstream from the reaction system, set at 3.6 MPa-g, which released the liquid effluent once the target pressure was attained. RCF conditions that yielded the best results in the batch runs were adapted to the FT system in the absence of H₂. Two conditions were used for 35-Mo₂C/AC, high and low catalyst loading (0.6 and 0.3 catalyst/biomass ratios, FT1 and FT2, respectively), whereas 5-Mo₂C/AC was only used at high catalyst loading level (see Table 2). The main results of these runs are summarized in Figure 3.

Code	Catalyst	Catalyst/ biomass	Flow (mL/min)	Time (min)
FT1	35-Mo ₂ C/AC	0.6	0.30/0.15	480/840
FT2	35-Mo ₂ C/AC	0.3	0.15	1320
FT3	5-Mo ₂ C/AC	0.6	0.15	1320

The mass of LDO from FT-RCF was almost constant in all FT processes: 46 ± 5 wt.%, 48 ± 2 wt.% and 52 ± 7 wt.% for FT1, FT2 and FT3 (Figure 3), while 44.4 ± 1.8 wt.% (where 1.8% accounts for the standard deviation) was achieved in the absence of catalyst. LDO in FT were very similar to that achieved in batch mode (*ca.* 51 wt.%). The measured monomer yield was 1.7 ± 0.1 wt.% in the absence of catalyst in FT processes.

This suggests that the degree of delignification is strongly dependent on the reaction temperature and the solvent flow, regardless of the catalyst load or its Mo₂C content.^[17,18] The average measured monomer yields presented some variability if consecutive runs were compared but, essentially the catalyst performance kept constant along the different runs (14.9 ± 2.9 wt.%, 14.2 ± 1.8 wt.% and 13.3 ± 3.4 wt.% average monomer yield for FT1 and FT2 and FT3 respectively, 95% confidence). For the sake of clarity, the results are presented as the average of three consecutive runs for 35-Mo₂C/AC (for complete detail of monomer yield and monomer distribution see figure S6). Monomer yields (around 15 wt.%) were significantly lower than that obtained in run 35d (34.7 wt.%), but much higher than those obtained in the absence of H₂, run 35e (8.7 wt.%). It is important to note that, in the FT system, hydrogenolysis can only take place *via* transfer hydrogenation from ethanol catalyzed by Mo₂C.^[22,27–31]

When 5-Mo₂C/AC was used (FT3), an average monomer yield of 13.3 ± 3.4 wt.% was attained, similar to those obtained using 35-Mo₂C/AC in FT2 and to the monomer yield obtained in the batch run using 5-Mo₂C/AC at 200 °C for 480 min under H₂ atmosphere (5d, 13.1 wt.%). In view of these results, it can be stated that FT-RCF offers clear advantages over batch RCF. The intensive contact between the solvolysis liquid stream and the catalyst allows conducting reductive fractionation in the absence of H₂.

The main difference between the results of these FT experiments lied on the products selectivities (Figure 3) and, more precisely, on the selectivity to reduced alkyl side chains. Thus, monomers S1, S3 and S4 accounted for 80 ± 5 wt.%, 61 ± 4 wt.% and 55 ± 6 wt.% in FT1, FT2 and FT3, respectively (see Table 2 for detailed conditions used in the FT experiments and Figure 2 for monomer identification). The cumulative amount of S1, S3 and S4 was constant for FT1 during the first 11 runs. In the case of FT2, this was only higher than 70 wt.% for the first two runs, whereas in runs 3–14 it decreased to 59 ± 3 wt.%, and kept constant for the rest of the runs. Noteworthy, this value is similar to that obtained in FT3, 55 ± 6 wt.%. In FT1 and FT2, S4 was the major phenolic monomer (43 ± 5 wt.% and 31 ± 2 wt.%, respectively) followed by S1 (31 ± 2 wt.% and 27 ± 2 wt.%, respectively), whereas in the case of FT3 the selectivity to S4 and S1 was similar (21 ± 8 wt.% and 25 ± 5 wt.%, respectively). It can be generally observed that the amount of reduced side-alkyl chains decreased with catalyst loading and catalyst runs, whereas the amount of monomers with an oxygen-containing side chain, acetosyringone (S7) and G5, increased. Indeed, the average amount of G5 increased from FT1 to FT2 and FT3 (1.3 ± 1.2 wt.%, 5.2 ± 0.8 wt.% and 10.6 ± 0.5 wt.% respectively).

The effect of the reaction conditions in FT was also noted in the product size distribution (Figure 3). SEC chromatograms for

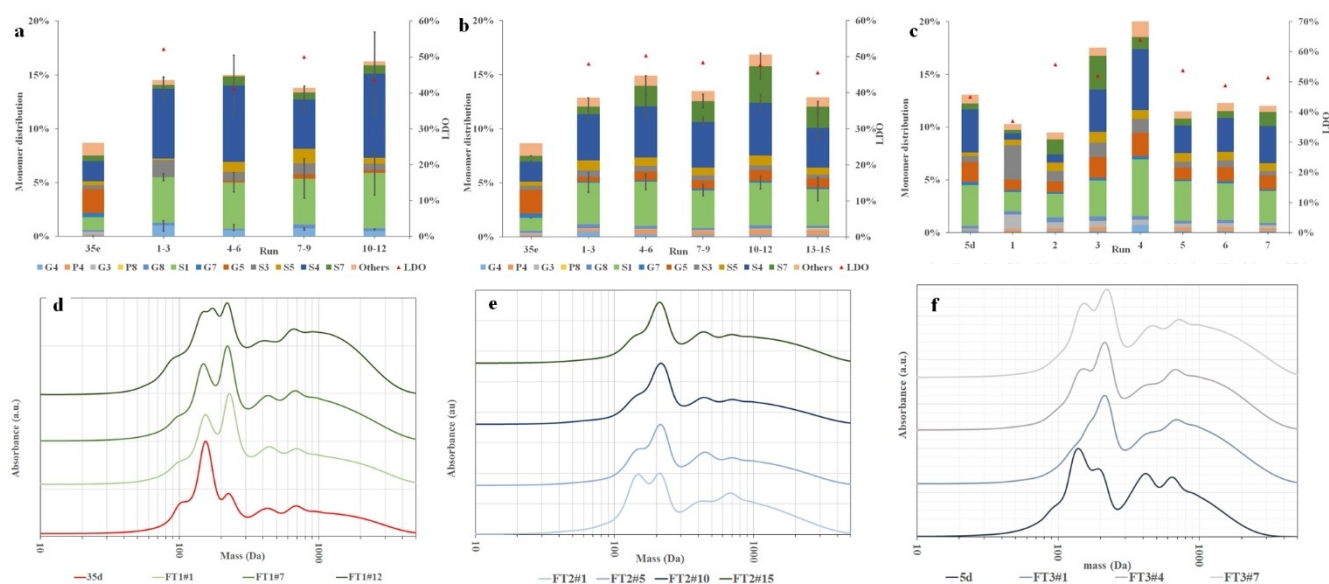


Figure 3. LDO yield and monomer distribution for flow-through RCF of poplar sawdust with 35-Mo₂C/AC at a) high catalyst loading (FT1) and b) low catalyst loading (FT2) and c) 5-Mo₂C/AC (FT3). Error bars correspond to the 95% confidence interval (significance level $\alpha = 0.05$, $n = 3$ replicates). SEC chromatograms for d) FT1 (runs #1, #7 and #12); e) FT2 (runs #1, #5, #10 and #15) and f) FT3 (runs #1, #4 and #7).

the first FT runs presented peaks corresponding to monomers (160 Da and 230 Da) that were accompanied by dimers and trimers (430 Da and 700 Da), and even shoulders at higher masses that are far more intense for FT3. The evolution of SEC chromatograms was similar in all FT processes. Monomers decreased their abundance with catalyst runs whereas higher masses became more significant. Noteworthy, even in the last FT-RCF runs, monomers were still the most prevalent species in all cases.

Similar information can be extracted from the aromatic regions of DOSY spectra. FT1 (Figure S7) presented diffusion traces at lower diffusion coefficients (*i.e.* higher apparent mass) with successive catalyst runs. Similarly, even from the first runs onwards it could be evidenced that traces corresponding to trimers and tetramers were present in FT2 (Figure S7d). Finally, DOSY spectra for FT3 was consistent with SEC. Apparent masses in FT3#1 were higher (275–1060 Da) than in FT1#1 and FT2#1, but no noticeable changes were observed in FT3#7 with regards to FT3#1.

Hetero single Quantum Coherence NMR (HSQC) analyses for ethanosolv lignin and LDO from batch and FT-RCF experiments presented cross-signals that could be assigned to aromatic moieties corresponding to syringyl, guaiacyl and hydroxyphenyl units.^[32,33] Furthermore, in the case of LDO obtained in batch RCF mode, a clear cross-signal at $\delta\text{C}/\delta\text{H}$ 131.5/6.25 ppm could be detected, which can be attributed to the unsaturation of the alkyl chain in S4 (Figure S8). As expected, the ratio of β -O-4 linkages, (estimated using HSQC extrapolated to time 0, HSQC₀, according to Table S4), slightly decreased from ethanosolv lignin to LDO obtained by RCF in batch mode (61% and 55%, respectively, Table S5) and kept constant around 50% in LDO obtained from FT runs.

Results from ³¹P NMR after derivatization with 2-chloro-4,4,5,5-tetramethyl-1,3,2-dioxaphospholane (TMDP, Table S6) indicated that the highest content of hydroxy groups was achieved in batch reactions with 35-Mo₂C/AC in ethanol at 200 °C (*ca.* 4.2 mmol/g, 2.8 mmol/g aromatic OH), which is consistent with the high proportion of phenolic monomers. FT reactions provided slightly lower values for FT3 (2.5 mmol/g aromatic OH) and FT1 and FT2 (1.8 mmol/g aromatic OH), which were constant along all the successive runs for each catalyst.

Hence, when batch RCF was carried at 200 °C in ethanol under H₂, 35-Mo₂C/AC (35d, Figure 1) presents much better catalytic performance than Ru/C and 5-Mo₂C/AC in terms of phenolic monomer yield (34 wt.%, 20 wt.% vs 13 wt.% respectively) that can be attributed to the relatively high molybdenum content. Similar monomer distribution was observed for 35-Mo₂C/AC and benchmark Ru/C. S1, S3 and S4 accounted for 80 wt.% of the monomers while decreasing to 40 wt.% in the absence of H₂ (35e) together with the production of 25 wt.% G5. When molybdenum content in the catalyst was reduced to 5 wt.%, 5-Mo₂C/AC, yields were only slightly lower than for Ru/C (13 wt.% vs 20 wt.% respectively). The main difference between 5-Mo₂C/AC and 35-Mo₂C/AC and Ru/C lied in the monomer distribution that was slightly different. Thus, when using 5-Mo₂C/AC a significant amount of G5 (14 wt.%) is produced, while G5 did not appear neither in the presence of 35-Mo₂C/AC

nor in the reaction catalyzed by Ru/C. This evidenced that, under similar conditions in batch reactions, the molybdenum content in the catalyst is important not only for the phenolic monomer yield but also for the selectivity of the reaction in terms of efficiency in the reduction of the alkyl side chain.

5-Mo₂C/AC and 35-Mo₂C/AC were compared in terms of monomer yield in FT-RCF mode. Average monomer yields in FT1 and FT2 were slightly higher than in FT3 (14.9 ± 2.9 wt.%, 14.2 ± 1.8 wt.% and 13.3 ± 3.4 wt.% respectively, 95 % confidence interval); however, opposite to that observed in batch mode, these differences could not be considered as relevant. This can be attributed to the different operation between batch and FT-RCF modes. In the case of batch mode, the catalyst, biomass, and solvent were mixed, and equilibria for solvodelignification and hydrogenolysis steps might be established. Additionally, it can be expected that diffusional limitations slowed-down both solvodelignification and hydrogenolysis and establish a clear difference in the RCF monomer yield depending on the catalyst loading in the batch reactor. However, under FT operation, the results obtained were accumulated ones from two-step non-equilibria processes, that is, the solvodelignification occurred by continuous flow of ethanol (consecutive extraction of lignin by fresh ethanol), whereas the conversion of lignin-derivatives from the first step via transfer hydrogenation occurred on the catalysts used as a second step of the process. This makes that those equilibria were shifted to the solvolysis of lignin and the hydrogenolysis of the solvolyzed lignin fragments. Furthermore, diffusional limitation are prevented as the FT compels the contact, first between the ethanol and the biomass feedstock, and second between solvolytic lignin and the catalyst.

As it was mentioned before, the main differences between 35-Mo₂C/AC and 5-Mo₂C/AC in FT-RCF were essentially found in the selectivity and, more specifically, in the reduction of the alkyl side chains. Selectivity in FT1 to S1 + S3 + S4 was similar than in the batch process under H₂ (35d) whereas a decrease in the selectivity was observed in FT2 and FT3. It is worth noting that this selectivity was still higher than in 35e and similar to 5d. This decrease in selectivity to S1 + S3 + S4 was accompanied by an increase in G5 from FT1 to FT2 and FT3. This indicated that the reduction of the alkyl side chain is less efficient when either the catalyst/biomass ratio decrease (FT1 and FT2) and when the molybdenum loading in the catalyst decrease (FT1 and FT3). Therefore, the effect of molybdenum loading in the catalyst seemed to be more relevant to complete the reduction of the alkyl side chain than for the monomer yield in the FT processes.

One of the main objectives of RCF is to preserve the saccharides in the parent lignocellulosic feedstock to use them in the production of fine chemicals.^[12,13] Signals corresponding to the anomeric carbon atoms from saccharides were clearly detected using NMR, both in the LDO and the aqueous phase from batch RCF reactions, while these signals were far less intense or directly not detected in samples from FT runs (Figure S9), which could be confirmed by High Pressure Liquid Chromatography (HPLC) analysis of the aqueous phases. These analyses did not show any signal corresponding to glucose or

xylose (Figure S9). The delignified pulp samples from batch RCF and from the cumulative of 7 runs in FT-RCF experiments were analyzed (see Table S7 and S1). A noticeable decrease in the cellulose content was observed in the pulp from batch reaction while it remained intact in the pulp after FT. The decrease in hemicelluloses can be explained by hydrolysis and autohydrolysis processes in the hemicellulose fraction, which can be promoted by the water present in the ethanolic solvent at the reaction temperatures.^[34] It has also been reported that hemicelluloses can play the role of internal reducing agents upon the solvolysis of lignin, which would contribute to their degradation.^[19,20]

FT processes clearly outperformed batch operation in terms of catalyst reuse. Phenolic monomer yield kept constant along the successive FT runs regardless of the reaction conditions considered, and only slight changes in the selectivity were noticed. In this sense, the increase of G5 and S7 can be seen as a symptom of catalyst deactivation. Additionally, both SEC and DOSY analyses evidenced that some catalyst deactivation took place with successive FT runs, as size distributions shifted to higher molecular masses in the LDO. Catalyst recyclability in FT may be hampered by the progressive activity decay caused by sintering, fouling and leaching.^[35] To this end, characterization of spent catalyst samples was carried out to gain insight on the main causes for catalyst deactivation, since very few studies tackle the fate of the catalyst after RCF processes.^[12,35,36] The presence of surface Mo (II) species in the spent catalysts was confirmed by XPS analyses (Table S8), and was consistent with the presence of surface Mo₂C species. Oxygen content in the surface was significantly higher in the spent catalyst (FT1#12) than in fresh 35-Mo₂C/AC. Additionally, the major contribution to 3d signals came from electrons corresponding to Mo 3d²/3d³, which are ascribed to surface Mo species having higher oxidation states than Mo (II).^[37] This higher oxidation states may eventually lead to the formation of Mo oxides as MoO₂ and MoO₃, which can be responsible for the increase of the amount of monomers with oxidized alkyl chain. Despite the presence of oxides, it is worth noting that XRD analyses (Figure S10) did clearly show the existence of β-Mo₂C phases in the spent catalyst, though.^[38] Therefore, it can be concluded that oxidation took place during the FT-RCF reactions, leading to Mo surface species, presumably Mo oxides, other than β-Mo₂C as evidenced by XPS measurements. It has been described that Mo₂C/ZrO₂ oxidation to MoO₂ occurred upon phenol hydrogenation^[39] which indicates that this surface oxidation may also occur in the surface of the catalysts used in the present work. These surface Mo oxides could be responsible for the increase of monomeric phenols with oxidized side chains, as it has been described for the RCF of herbaceous biomass using a MoO₂/AC catalyst, being coumarates and ferulates the predominant monomers.^[40]

The loss of Mo from the catalysts by leaching could be confirmed by the presence of Mo in the LDO, according to the ICP-OES results. The amount of Mo in the LDO was much lower in FT (250–570 ppm, Table S9) than in batch RCF run 35d (6,330 ppm). Mo content in LDO was higher in the first runs of FT2 and FT3 (1,607 ppm and 570 ppm, respectively) than in the

last runs (213 ppm and 250 ppm, respectively), while it kept constant along FT1 runs. Mo content was, as expected, higher in LDO from FT1 than from FT2 and FT3, because of the highest solvent flowrate and catalyst load. Consequently, biomass ethanolysis rates were higher, and subsequently the phenolics flowrate contacting the catalytic bed too, which increased metal leaching. The flowrate effect was also noticed in the Mo content in the spent catalyst (Table S9). The Mo content was 6 wt.% measured after the FT1#12 run, and 19 wt.% after the FT2#15 run. This indicates that in FT1 almost 83% of the Mo in the catalyst was leached throughout, whereas in the case of FT2, more than 54% of the starting Mo remained in the catalyst. Similarly, the Mo content after FT3#7 decreased to 2.8%, showing that only 43% of the Mo was leached after 7 consecutive runs. Certainly, these Mo values are not optimal in FT runs. However, it must be noticed that ca. 20% Mo leaching has been reported in the catalytic hydrogenolysis of lignin using MoO₂ in batch mode.^[41]

High Resolution Transmission Electron Microscopy (HR-TEM) images from the spent samples (Figure S11) were consistent with some Mo leaching. Opposite to what was observed in the fresh catalyst, large agglomerates were not encountered. Indeed, discrete nanoparticles were observed in FT1#12 having a narrow size distribution around 4–11 nm and an average particle size of 6.0 ± 0.3 nm, whereas in the case of FT2#15 this average particle size was 10.9 ± 0.7 nm and the size distribution was broader (5–23 nm). This can be attributed to the removal of less stable Mo₂C particles on the AC surface. In both cases, lattice fringes corresponding to Mo₂C and graphite were observed, and the presence of Mo and C was confirmed by EDS. Finally, large agglomerates of inorganic salts that may come from feedstock ashes were observed in the spent catalyst (Figure S12). These agglomerates may also contribute to catalyst deactivation.

It can be assumed that metal leaching in FT-RCF processes is mainly caused by the interaction of the catalyst with the solvent, together with phenolic and oligophenolic compounds in the early stages of their interaction with the active metal.^[38] It has to be highlighted that no external H₂ was supplied in the FT-RCF reactions, thus hydrogenolysis occurs *via* transfer hydrogenation using ethanol that involves a catalytic cycle through high oxidation states, which contributes to the surface Mo oxidation. The solubilization of Mo oxides having a low degree of interaction with the AC support instead of Mo present as Mo₂C can be seen as the main cause for Mo leaching.

Conclusions

Flow-Through Reductive catalytic fractionation (FT-RCF) is a promising strategy for obtaining renewable phenolics from lignocellulosic residues following a 'lignin-first' biorefinery approach. β-Mo₂C/AC has shown excellent performance both in batch RCF and flow-through configurations. Under the studied conditions, the 35-Mo₂C/AC catalyst tested in batch RCF yielded almost double of the monomers obtained with a commercial Ru/C catalyst with very similar monomer distributions, while 5-

Mo₂C/AC presented a slightly lower monomer yield. 35-Mo₂C/AC and 5-Mo₂C/AC were also tested in FT mode for the RCF of poplar sawdust, without any H₂ gas co-fed. Monomer production was higher than in batch RCF without H₂. This outlines that hydrogenolysis of solubilized lignin fragments into monomers occurs *via* transfer hydrogenation from ethanol. To this end, FT configuration is convenient, as it enhances the contact between solubilized lignin fragments and the catalyst bed, which increases the transfer hydrogenation reaction, producing similar monomer yields than those attained in the batch mode. Oxidation of the surface Mo₂C active phase into Mo oxides during the transfer hydrogenation has been detected, which seems to favor Mo leaching. This can play an important role in the evolution of the catalytic performance at the long-term. Further work must be done to tackle the problem of the active phase leaching, which will require of a dedicated study to explore viable strategies to stabilize the Mo active phase.

FT reaction mode allowed easy recovery of the delignified pulp that preserved most of its holocellulose content. RCF catalysts were easily recovered too, and up to 15 consecutive runs have been carried out successfully, without a significant loss of activity and selectivity, which is the most extensive catalyst recycling in FT-RCF of biomass reported to date without catalyst regeneration.

Hence, the results obtained using the low-cost β-Mo₂C/AC catalyst in FT-RCF mode can be regarded as promising although some improvements must be done. Efforts to improve the carburization stage and to find the optimal Mo loading that results in highly active and stable Mo₂C supported catalysts are underway and will constitute the subject of future studies. The continuous feeding of biomass to the RCF reactor for attaining a true continuous process should also be explored to ensure better scaling-up and improve the viability of the lignin-first strategy at relevant industrial scales.

Experimental Section

Catalyst preparation

Catalysts were synthesized by incipient wetness impregnation of an ammonium heptamolybdate solution in deionized H₂O on AC followed by carburization under hydrogen flow and by surface passivation. AC (2.75 g) was impregnated with 5 mL of an ammonium heptamolybdate tetrahydrate (0.055 g/mL, 0.044 mmol/mL for 5-Mo₂C/AC, and 0.552 g, 0.446 mmol/mL for 35-Mo₂C/AC). Impregnation was made in three successive steps (2.0 mL, 1.5 mL and 1.5 mL). After each impregnation step, the solid was oven dried for 1 h at 105 °C. Finally, the impregnated AC were subjected to carburization under hydrogen atmosphere at 750 °C, according to the procedure described by Li *et al.*^[42] and to surface passivation at room temperature. The catalysts were characterized by Inductively Coupled Plasma to Optical Emission Spectroscopy, (ICP-OES), Scanning Transmission Electron Microscopy combined with energy-dispersive spectroscopy (STEM-EDS), X-Ray photoelectron spectroscopy (XPS) and X-Ray diffraction (XRD). For further characterization details please see the Supporting Information (SI).

Lignin Reductive Catalytic Fractionation tests.

Batch RCF reactions were carried out in an Autoclave Engineers reaction system (EZ100RXR) having a 100 mL AISI 316 stainless steel pressurized vessel as reactor, equipped with a PID temperature controller and a mechanical stirrer. Poplar sawdust (3,500 mg) and β-Mo₂C/AC (5 wt.% or 35 wt.% Mo, 500 mg) or Ru/C (5 wt.% Ru, 525 mg) were suspended in the solvent of choice (70 mL) and set in the stainless-steel vessel. The reactor was purged (thrice with N₂ and H₂) and finally pressurized with hydrogen at 1 MPa-g. Reaction time started upon reaching the target temperature. After the reaction, the reactor was allowed to cool down and the resulting suspension was filtered. The solid was thoroughly washed with ethanol and concentrated by rotary vacuum distillation. The resulting oil was treated with an aqueous solution of HCl (pH 2, 25 mL) and a solution of bromobenzene (0.0015 M, 25 mL) in ethyl acetate. The organic phase was then separated. 1.0 mL of the organic phase was taken for the quantification of monomeric phenols by GC-FID. The rest was evaporated to dryness and the yield to lignin-derived oil (LDO) was gravimetrically calculated. LDO was characterized by SEC and NMR. For further details, please see the SI.

FT reactions were done in a pressurized experimental setup at laboratory scale. The FT system (Figure SI 5) was composed of a liquid feeding system (JASCO PU-1585 HPLC pump) and two AISI 316 stainless-steel tubular reactors connected in series for placing two separate beds, both having a fixed-bed reactor configuration (the first for the biomass feedstock, and the second for the catalyst bed). These reactors are placed inside a column oven (JASCO RO-4068) having a built-in temperature controller. The pressure was controlled using a back-pressure regulator (JASCO BP-1580-81) downstream from the reaction system, set at 3.6 MPa-g, which released the liquid effluent once the target pressure was attained.

The feedstock bed, *ca.* 975 mg of poplar sawdust, was placed in a 1/2-inch o.d. tube with 10.0 mm i.d. and 100 mm of length (7.85 mL). The catalyst bed was loaded into a 49 mm long tube (3.92 mL) having the same o.d. as the former (see figure S1). Two different experiments were carried out with 35-Mo₂C/AC at different catalyst loadings (Table 2): high (585 mg) and low (299 mg) catalyst loading, resulting in catalyst-to-biomass mass ratios of 0.6 and 0.3, respectively, denoted as FT1 and FT2 tests. The 5-Mo₂C/AC catalyst (580 mg) was also tested using a catalyst-to-biomass ratio of 0.6 (FT3). The reaction temperature was fixed at 195 °C and continuously monitored inside the catalyst bed by means of a K-type thermocouple connected to a digital thermometer (1319 A K-type, RS Amidata). The thermosensitive tip of the thermocouple was placed inside the catalytic bed. In the FT1 test, ethanol was flown at variable liquid flow rates (0.30 mL/min for 8 h followed by 0.15 mL/min for 14 h), whereas a constant flow rate of 0.15 mL/min was held for 22 h in the FT2 and FT3 tests, resulting in a total of 198–270 mL per run. Then, the system was allowed to cool down and the biomass feedstock bed was replaced with another fresh sample. Each replacement of biomass was regarded as a different run, and the liquid product samples of the different runs were analysed separately. Hereafter, the runs will be denoted as FTn#m, with n being the kind of test (1, 2 or 3) and m the number of runs. The samples of the different runs were collected, the ethanolic solutions were concentrated by rotary distillation, then treated with an aqueous solution of HCl (pH 2, 25 mL) and then extracted with ethyl acetate (25 mL). The organic layer was separated from the aqueous phase, treated with magnesium sulphate and the solvent was evaporated to complete dryness. Monomer yields are given against the total mass of lignin in the biomass feedstock (Table S3 in the SI), and are presented as cumulative yields of phenolic monomers (Table S11) in the case of FT runs.

Characterization of the reaction products after RCF tests was carried out using different techniques, including gas chromatography with flame ionization detector (GC-FID) or coupled to mass spectrometry (GC-MS), size exclusion chromatography (SEC), and nuclear magnetic resonance (NMR). Detailed information about the different chemicals, biomass feedstock, catalyst characterization and analytical methods used in the characterization of the liquid products can be found in the SI.

Supporting Information

Supporting Information is available from the Wiley Online Library

Acknowledgements

Authors would like to acknowledge the use of the Servicio General de Apoyo a la Investigación-SAI, Universidad de Zaragoza (UNIZAR), especially Dr. Ana Guitart and the rest of the staff of the Servicio de Análisis Químico for the ICP-OES analyses, as well as the use of the services by the Laboratorio de Microscopías Avanzadas (LMA) that also belongs to SAI-UNIZAR. More specifically, Dr. Alfonso Ibarra and Dr. Guillermo Antorrena are acknowledged for the STEM/HRTEM-EDS and XPS analyses respectively. Staff from UPNA's Unidad Científico-Técnica de Apoyo a la Investigación (UCTAI), are also greatly acknowledged for their support in the use of the GC-MS and XRD equipments. M.M. and K.H. are very grateful to the Universidad Pública de Navarra (UPNA) for their PhD grants. F.B. wishes to thank J. Arch and J. Mattheos for providing inspiration during the preparation of this manuscript. AC wishes to thank to L. Arce for her infinite patience and support. This research was funded by the Gobierno de Navarra, grant number PC177-178 Reducenano 2.0 and Spanish Ministry of Science (AbFine, PID2020-114936RB-I00). The APC was funded by the Universidad Pública de Navarra (UPNA).

Conflict of Interests

The authors declare no conflict of interest.

Data Availability Statement

This Research article is published in Open Access, so that the data contained herein are accessible.

Keywords: Poplar native lignin · molybdenum carbide · reductive catalytic fractionation · flow-through reactor

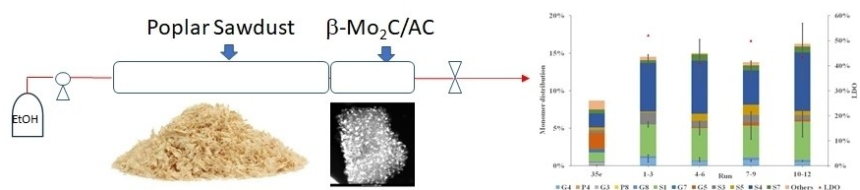
- [1] B. Gómez-Monedero, M. P. Ruiz, F. Bimbela, J. Faria, *Appl. Catal. A* **2017**, *541*, 60–76.
 [2] B. H. Davison, J. Parks, M. F. Davis, B. S. Donohoe, in *Aqueous Pretreatment of Plant Biomass for Biological and Chemical Conversion to Fuels and Chemicals*, John Wiley & Sons, Ltd, Chichester, UK, **2013**, pp. 23–38.

- [3] J. E. Bidlack, W. V. Dashek, in *Plant Cells and Their Organelles*, John Wiley & Sons, Ltd, Chichester, UK, **2016**, pp. 209–238.
 [4] A. García, M. González Alriols, J. Labidi, *Ind. Crops Prod.* **2014**, *53*, 102–110.
 [5] H. Wang, Y. Pu, A. Ragauskas, B. Yang, *Bioresour. Technol.* **2019**, *271*, 449–461.
 [6] A. Cornejo, I. Alegria-Dallo, Í. García-Yoldi, Í. Sarobe, D. Sánchez, E. Otazu, I. Funcia, M. J. Gil, V. Martínez-Merino, *Bioresour. Technol.* **2019**, *288*, 121583.
 [7] S. Van Den Bosch, W. Schutyser, R. Vanholme, T. Driessen, S. F. Koelewijn, T. Renders, B. De Meester, W. J. J. Huijgen, W. Dehaen, C. M. Courtin, B. Lagrain, W. Boerjan, B. F. Sels, *Energy Environ. Sci.* **2015**, *8*, 1748–1763.
 [8] T. Renders, G. Van den Bossche, T. Vangeel, K. Van Aelst, B. Sels, *Curr. Opin. Biotechnol.* **2019**, *56*, 193–201.
 [9] H. D. Thi, K. Van Aelst, S. Van den Bosch, R. Katahira, G. T. Beckham, B. F. Sels, K. M. Van Geem, *Green Chem.* **2022**, *24*, 191–206.
 [10] A. Kramarenko, D. Etit, G. Laudadio, F. Neira D'Angelo, *ChemSusChem* **2021**, *14*, 3838–3849.
 [11] K. Zhang, H. Li, L.-P. Xiao, B. Wang, R.-C. Sun, G. Song, *Bioresour. Technol.* **2019**, *285*, 121335.
 [12] S. Van den Bosch, T. Renders, S. Kennis, S. F. Koelewijn, G. Van Den Bossche, T. Vangeel, A. Deneyer, D. Depuydt, C. M. Courtin, J. M. Thevelein, W. Schutyser, B. F. Sels, *Green Chem.* **2017**, *19*, 3313–3326.
 [13] A. W. Bartling, M. L. Stone, R. J. Hanes, A. Bhatt, Y. Zhang, M. J. Bidy, R. Davis, J. S. Kruger, N. E. Thornburg, J. S. Luterbacher, R. Rinaldi, J. S. M. Samec, B. F. Sels, Y. Román-Leshkov, G. T. Beckham, *Energy Environ. Sci.* **2021**, *14*, 4147–4168.
 [14] O. Y. Abdelaziz, K. Li, P. Tunã, C. P. Hultberg, *Biomass Convers. Biorefinery* **2018**, *8*, 455–470.
 [15] F. Brandi, M. Antonietti, M. Al-Naji, *Green Chem.* **2021**, *23*, 9894–9905.
 [16] E. M. Anderson, M. L. Stone, R. Katahira, M. Reed, G. T. Beckham, Y. Román-Leshkov, *Joule* **2017**, *1*, 613–622.
 [17] E. M. Anderson, M. L. Stone, M. J. Hu, G. T. Beckham, Y. Roma, *ACS Sustainable Chem. Eng.* **2018**, *6*, 7951–7959.
 [18] E. M. Anderson, M. L. Stone, R. Katahira, M. Reed, W. Muchero, K. J. Ramirez, G. T. Beckham, Y. Román-Leshkov, *Nat. Commun.* **2019**, *10*, 2033.
 [19] I. Kumaniaev, E. Subbotina, J. Sävmarker, M. Larhed, M. V. Galkin, J. S. M. Samec, *Green Chem.* **2017**, *19*, 5767–5771.
 [20] I. Kumaniev, E. Subbotina, M. V. Galkin, P. Srifa, S. Monti, I. Mongkolpichayarak, D. N. Tungasmita, J. S. M. Samec, *Pure Appl. Chem.* **2020**, *92*, 631–639.
 [21] R. Ma, W. Hao, X. Ma, Y. Tian, Y. Li, *Angew. Chem. Int. Ed.* **2014**, *53*, 7310–7315.
 [22] K. Wu, C. Yang, Y. Zhu, J. Wang, X. Wang, C. Liu, Y. Liu, H. Lu, B. Liang, Y. Li, *Ind. Eng. Chem.* **2019**, *58*, 20270–20281.
 [23] S. Qiu, X. Guo, Y. Huang, Y. Fang, T. Tan, *ChemSusChem* **2019**, *12*, 944–954.
 [24] A. Cornejo, F. Bimbela, R. Moreira, K. Hablich, Í. García-Yoldi, M. Maisterra, A. Portugal, L. M. Gandía, V. Martínez-Merino, *Biomol. Eng.* **2020**, *10*, 1–30.
 [25] S. Qiu, M. Wang, Y. Fang, T. Tan, *Sustain. Energy Fuels* **2020**, *4*, 5588–5594.
 [26] W. Schutyser, S. Van den Bosch, T. Renders, T. De Boe, S. F. Koelewijn, A. Dewaele, T. Ennaert, O. Verkinderen, B. Goderis, C. M. Courtin, B. F. Sels, *Green Chem.* **2015**, *17*, 5035–5045.
 [27] H. Xu, H. Li, *J. Energy Chem.* **2022**, *73*, 133–159.
 [28] M. M. Sullivan, J. T. Held, A. Bhan, *J. Catal.* **2015**, *326*, 82–91.
 [29] Y. S. Yun, C. E. Berdugo-Díaz, D. W. Flaherty, *ACS Catal.* **2021**, *11*, 11193–11232.
 [30] M. Shetty, E. M. Anderson, W. H. Green, Y. Román-Leshkov, *J. Catal.* **2019**, *376*, 248–257.
 [31] W.-S. Lee, Z. Wang, R. J. Wu, A. Bhan, *J. Catal.* **2014**, *319*, 44–53.
 [32] B. N. Kuznetsov, N. V. Chesnokov, I. G. Sudakova, N. V. Garyntseva, S. A. Kuznetsova, Y. N. Malyar, V. A. Yakovlev, L. Djakovitch, *Catal. Today* **2018**, *309*, 18–30.
 [33] J. L. Wen, S. L. Sun, B. L. Xue, R. C. Sun, *Materials* **2013**, *6*, 359–391.
 [34] W. Sebhat, A. El-roz, A. Crepet, C. Ladavière, D. Da, S. Perez, S. Mangematin, C. C. Almada, L. Vilcoq, L. Djakovitch, P. Fongarland, *Biomass Convers. Biorefinery* **2020**, *10*, 351–366.
 [35] E. O. Ebikade, N. Samulewicz, S. Xuan, J. D. Sheehan, C. Wu, D. G. Vlachos, *Green Chem.* **2020**, *22*, 7435–7447.
 [36] X. Liu, H. Li, L.-P. Xiao, R.-C. Sun, G. Song, *Green Chem.* **2019**, *21*, 1498–1504.

- [37] J. Baltusaitis, B. Mendoza-Sanchez, V. Fernandez, R. Veenstra, N. Dukstiene, A. Roberts, N. Fairley, *Appl. Surf. Sci.* **2015**, *326*, 151–161.
- [38] A. Navajas, I. Reyero, E. Jiménez-Barrera, F. Romero-Sarria, J. Llorca, L. M. Gandía, *Catalysts* **2020**, *10*, 158.
- [39] P. M. Mortensen, H. W. P. de Carvalho, J.-D. Grunwaldt, P. A. Jensen, A. D. Jensen, *J. Catal.* **2015**, *328*, 208–215.
- [40] X. Gong, J. Sun, X. Xu, B. Wang, H. Li, F. Peng, *Bioresour. Technol.* **2021**, *333*, 124977.
- [41] L. P. Xiao, S. Wang, H. Li, Z. Li, Z. J. Shi, L. Xiao, R. C. Sun, Y. Fang, G. Song, *ACS Catal.* **2017**, *7*, 7535–7542.
- [42] X. Li, D. Ma, L. Chen, X. Bao, *Catal. Lett.* **2007**, *116*, 63–69.
- [43] A. Sluiter, B. Hames, R. Ruiz, C. Scarlata, J. Sluiter, D. Templeton, *Lab. Anal. Proced. NREL/TP-510-42623* **2008**, 1–14.
- [44] I. Sádaba, M. Ojeda, R. Mariscal, M. L. Granados, *Appl. Catal. B* **2014**, *150–151*, 421–431.
- [45] S. Van Den Bosch, W. Schutyser, S. F. Koelewijn, T. Renders, C. M. Courtin, B. F. Sels, *Chem. Commun.* **2015**, *51*, 13158–13161.
- [46] L. A. Colón, L. J. Baird, *Techniques and Instrumentation, in Modern practice of gas chromatography* (Eds.: R. L. Grob, E. F. Barry), Wiley & Sons, **2004**, pp 275–337.
- [47] K. Hu, W. M. Westler, J. L. Markley, *J. Am. Chem. Soc.* **2011**; *133*, 1662–1665.
- [48] Y. Pu, S. Cao, A. J. Ragauskas, *Energy Environ. Sci.* **2011**, *4*, 3154–3166.

Manuscript received: November 3, 2023
Revised manuscript received: December 19, 2023
Accepted manuscript online: January 5, 2024
Version of record online: ■■, ■■

RESEARCH ARTICLE



A Flow-Through reactor has been set for the Reductive Catalytic Fractionation of lignocellulose using $\beta\text{-Mo}_2\text{C}/\text{AC}$ as catalyst. The catalysts could be used in up to 15 cycles keeping both

its activity and selectivity. Activity and selectivity to reduced side-alkyl chain in the FT configuration outperformed those achieved in the batch configuration under similar conditions.

M. Maisterra, M. Atienza-Martínez, K. Hablich, R. Moreira, V. Martínez-Merino, L. M. Gandía, A. Cornejo, F. Bimbela**

1 – 11

Innovative flow-through reaction system for the sustainable production of phenolic monomers from lignocellulose catalyzed by supported Mo_2C .

